

Effect of hydrogen on plastic strain localization and failure in single crystals of austenitic stainless steel

Lev B. Zuev^a, Svetlana A. Barannikova^b

Institute of Strength Physics and Materials Science, SB RAS

2/4, Akademicheskii Ave., Tomsk, 634021, Russia

^albz@ispms.tsc.ru, ^bbsa@ispms.tsc.ru

Keywords: Hydrogen-induced plastic strain localization, failure

Abstract. The effect of interstitial hydrogen atoms on the mechanical properties and plastic strain localization patterns in tensile tested Fe–18Cr–12Ni–2Mo single crystals of austenite steel with low stacking-fault energy has been studied using a double exposure speckle photography technique. The main parameters of plastic flow localization at various stages of the deformation hardening of crystals have been determined in single crystals of steel electrolytically saturated with hydrogen in a three electrode electrochemical cell at a controlled constant cathode potential.

Introduction

Previously, we presented experimental data [1–3] according to which plastic strain development in solids exhibited a localized character over the entire process. This phenomenon is especially clearly manifested on a macroscopic scale, where the patterns of strain localization are related to the deformation hardening operative on the corresponding stages of straining. In this case, the observed patterns acquire the form of autowaves of various types, and there is a uniquely relation ship between the autowave type and the law of strain hardening at this stage of plastic flow in single crystals. Solid solutions based on fcc iron constitute a basis for stainless steels that are promising construction materials. As is known, the hydrogenation of polycrystalline austenitic steels leads to their accelerated brittle fracture [4]. This phenomenon poses a serious practical problem, the solution of which determines the durability and safety of operation of a steel structure. The main aim of this investigation was to elucidate the effect of dissolved hydrogen on the macroscopic plastic flow localization patterns in tensile strained chromium–nickel austenite single crystals, i.e., under conditions not complicated by the presence of grain boundaries.

The experimental conditions and materials

The experiments were performed on Fe–18Cr–12Ni–2Mo single crystals of austenite steel with low stacking-fault energy ($\gamma_0 = 0.02 \text{ J/m}^2$ [5]) that were grown using the Bridgman technique. The initial single-crystalline ingot was homogenized for 50 h at 1473 K. Then, standard dumbbell samples were cut using an electric-erosion tool, annealed in a helium atmosphere for 1h at 1373 K, and quenched from this temperature in water. The samples had a working part with dimensions of $25 \cdot 5 \cdot 1 \text{ mm}$, where the wide face coincided with the (110) plane and the longitudinal axis coincided with the $[\bar{1}11]$ direction. Single crystals with the longitudinal axis oriented in this direction have six $\langle 110 \rangle\{111\}$ slip systems with the same Schmid factor of $m \approx 0.27$. The samples were tensile strained at 300 K on an Instron Model 1185 testing machine at a mobile clamp velocity of $3.3 \cdot 10^{-6} \text{ m/s}$. The distributions of the plastic distortion tensor components for all points of the sample surface were determined using the method of double-exposure speckle photography (DESP) [3]. The structure of single crystals was examined in a Neophot-21 optical microscope. The single-crystalline steel samples were electrolytically saturated with hydrogen in a thermostatted three-electrode electrochemical cell with graphite anode, operating at a controlled constant cathode potential of $U = -500 \text{ mV}$ (relative to silver chloride reference electrode) in a 1 N sulfuric acid solution containing

20 mg/l thiourea. The hydrogenation was effected at 323 K for 70 h after preliminary purging the solution with nitrogen. The current–voltage curves were recorded using an IPC-Compact potentiostat. The hydrogen concentration was ~50 wt ppm was evaluated using a method [6] based on an empirical dependence that took into account the conditions of potentiostatic electrolytic hydrogenation (cathode over potential, temperature and duration of the hydrogen saturation and subsequent annealing), sample thickness, and hydrogen diffusion coefficient in austenite stainless steel. The electrolytic hydrogenation of single crystals of steel in the three-electrode electrochemical cell at a constant cathode potential ensures a more uniform distribution of hydrogen over the sample thickness compared to the traditional method of electrochemical saturation at a constant current density [7]. Prior to mechanical testing, the samples were kept in liquid nitrogen.

Localization patterns of plastic deformation

We have studied the evolution of patterns of the plastic flow macrolocalization in austenite stainless steel single crystals in the initial state and upon the saturation of the electrolytic with hydrogen. In $[\bar{1}11]$ oriented single crystals of Fe–18Cr–12Ni–2Mo austenite steel, the plastic flow proceeds via dislocation shifts and, hence, multiple slippage can be expected.

On the stress–strain (σ – ε) curve of plastic flow measured in tension for austenite stainless steel single crystals in the initial (hydrogen-free) state, the transition from elasticity to developed plastic flow is followed by the stages of (II) linear deformation hardening with a constant coefficient of $\theta \approx 960$ MPa, which extends to a total strain of $\varepsilon_{\text{tot}} = 0.03$ – 0.14 , and (III) parabolic (Taylor’s) hardening with a power index of $n = 1/2$, which extends up to $\varepsilon_{\text{tot}} = 0.4$. The fracture occurs by cutting and is accompanied by the formation of a neck in the middle part of the sample. The main mechanism of plastic straining in the initial $[\bar{1}11]$ oriented single crystals is multiple slippage, which determines the character of stages on the plastic flow curves [5].

The $\sigma(\varepsilon)$ curves of single crystals of austenite stainless steel saturated with hydrogen to a concentration of ~50 wt ppm exhibit a small tooth and a flow trough (I) that extends up to $\varepsilon_{\text{tot}} = 0.01$ and is followed by the stages of (II) linear deformation hardening with a constant coefficient of $\theta \approx 1000$ MPa, which extends to a total strain of $\varepsilon_{\text{tot}} = 0.02$ – 0.17 ; (III) parabolic (Taylor’s) hardening with a power index of $n = 1/2$, which extends up to $\varepsilon_{\text{tot}} = 0.18$ – 0.4 ; and (IV) prefracture with $n < 1/2$, which extends up to $\varepsilon_{\text{tot}} = 0.55$. In this case, the fracture takes place without neck formation and the crack develops in the direction perpendicular to the axis of tension. The entire plastic flow curve shifts downward relative to that for the austenite stainless steel single crystals in the initial (hydrogen-free) state. Thus, the hydrogenation of $[\bar{1}11]$ oriented single crystals of Fe–18Cr–12Ni–2Mo steel led to a decrease in the yield stress, 1.3-fold increase in the plasticity (strain at break), and suppression of the neck formation in single crystals oriented for the multiple slippage [8].

Hydrogenation decreases the stacking fault energy in the studied alloy, which leads to an increase in the splitting of dislocations for tensile-strained crystals with orientations near the $[\]$ pole of the stereographic triangle. This circumstance facilitates the development of plastic shear and its localization in one of the six equiprobable $\langle 110 \rangle \{111\}$ slip systems, which apparently accounts for the appearance of a small tooth and flow trough. At the same time, the saturation with hydrogen almost does not change the coefficient of deformation hardening in the linear stage, which is typical of specially doped fcc materials [9]. This behavior is related to the development of a planar structure of flat dislocation pileups in the initial state, which is not significantly changed by subsequent hydrogenation [8].

The measurements of local strain distributions using the DESP method showed that the strain is macroscopically localized at all stages of plastic flow in single crystals of austenite stainless steel. An analysis of these patterns revealed that, in the initial (hydrogen-free) state of crystals, the tensile plastic strain at the stage of linear deformation hardening (II) is concentrated within local zones

spaced by a distance of $\lambda = 4 \pm 1$ mm (Fig. 1a). These local strain zones (autowaves) moved at a velocity of $V_{aw} = 3.5 \cdot 10^{-5}$ m/s, which was determined from the slope of the $X(t)$ curves (Fig. 2a) that plot the positions X of maxima of the ε_{xx} strain component on the axis of straining as functions of time t . At the stage of parabolic deformation hardening (III), the system of equidistant strain localization zones becomes stationary, then these immobile foci of plastic strain localization start to move consistently with a tendency to merge together at the middle of a sample, where the fracture takes place.

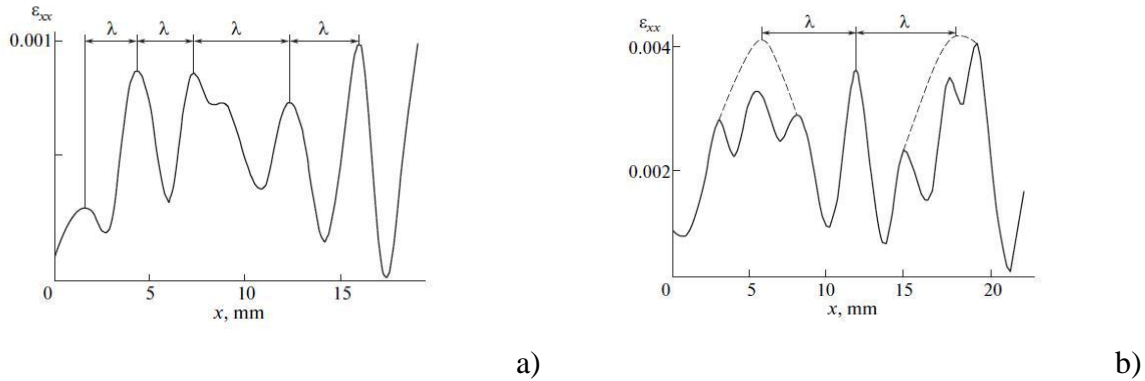


Fig. 1. Pattern of strain distribution plotted as the local elongation component $\varepsilon_{xx}(x)$ along axis of tension at stage of linear deformation hardening (II) at a total strain of $\varepsilon_{tot} = 0.05$ in $[\bar{1}11]$ oriented single crystal of Fe–18Cr–12Ni–2Mo austenite steel (a) in the initial state (free of interstitial impurity atoms) and (b) upon the electrolytic saturation with hydrogen at $U = -500$ mV in 1 N aqueous H_2SO_4 for 70 h at $T = 323$ K.

An analysis of the distributions of local strain ε_{xx} in tensile tested single crystals of austenite stainless steel saturated hydrogen to 50 wt ppm showed that, in this case, a single zone of localized straining was formed on the flow trough (I), which separated the strained and unstrained parts of the sample. At the stage of linear deformation hardening (II), the pattern of plastic strain localization represented a set of wide zones, each of which contains two to three related local strain foci. The zones exhibited a characteristic spacing of $\lambda = 6.5 \pm 1$ mm (Fig. 1b). These local straining zones (autowaves) also moved at a velocity of $V_{aw} = 2.5 \cdot 10^{-5}$ m/s (Fig. 2b). At the stage of parabolic deformation hardening (III), the system of wide strain localization zones became stationary. At the prefracture stage (IV), the immobile foci of plastic strain localization started moving consistently with a tendency to merge into a high-amplitude focus of localized straining, where a neck-like narrowing of the sample cross section was formed. When an ultimate stress level was attained, this focus began to move at a velocity of $V_{aw} = 3.0 \cdot 10^{-5}$ m/s toward the mobile clamp of the testing machine. Thus, in hydrogen-saturated samples, the crack nucleated near the mobile clamp. This character of the development of the pattern of strain macrolocalization at the stage of prefracture was observed for the first time. Previously [1], the motion of a single zone of strain localization was observed only at the initial stage of deformation hardening in fcc single crystals, e.g., on a flow trough or easy glide stage, where the plastic flow proceeded in a primary slippage/twinning system. It can be suggested that the hydrogen doping of $[\bar{1}11]$ oriented single crystals of Fe–18Cr–12Ni–

2Mo austenite steel led to enhanced local straining by slippage in one of the six equiprobable $\langle 110 \rangle \{111\}$ slip systems and suppressed the initial neck formation in the middle part of the sample. Metallographic analysis of the sample macrostructure at the state of prefracture showed that strain bands were formed on the surface of Fe–18Cr–12Ni–2Mo austenite steel single crystal. The average width of these bands, which was determined by the method of secants [10], amounted to $490 \pm 190 \mu\text{m}$ for samples in the initial state and $700 \pm 210 \mu\text{m}$ for samples upon the electrolytic saturation with hydrogen.

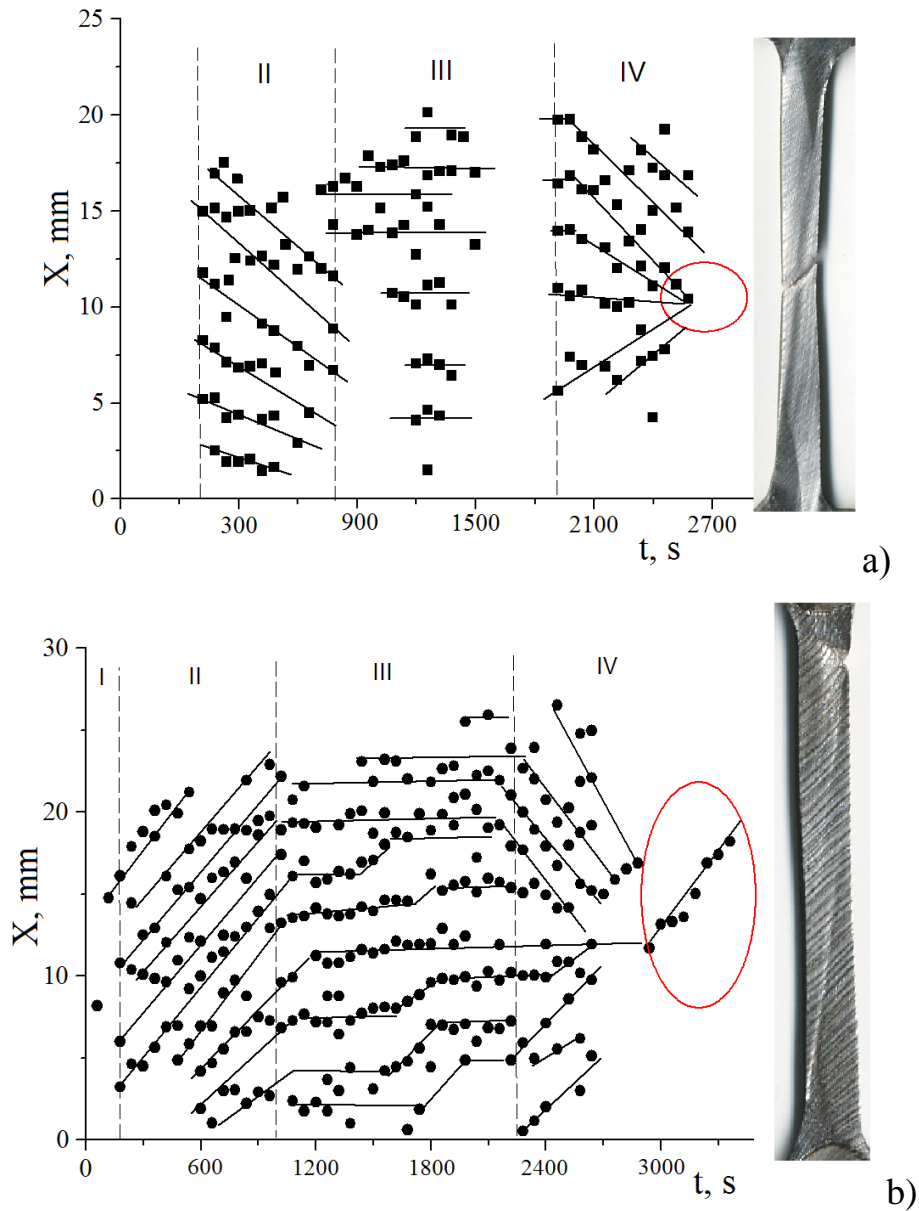


Fig. 2. Plots of positions $X(t)$ of strain localization foci along sample axis as functions of time at various stages of deformation hardening in $[\bar{1}11]$ oriented single crystal of Fe–18Cr–12Ni–2Mo austenite steel (a) in initial state (free of interstitial impurity atoms) and (b) upon electrolytic saturation with hydrogen at $U = -500$ mV in 1 N aqueous H_2SO_4 for 70 h at $T = 323$ K. Pole of fracture is indicated by an oval.

Summary

Thus, we have elucidated the effect of hydrogen on the macroscopic patterns of plastic strain localization in tensile tested $[\bar{1}11]$ oriented single crystals of Fe–18Cr–12Ni–2Mo austenite steel. It is established that the hydrogenation enhances the localization of straining leads to significant changes in the characteristic distances between plastic shear bands and local straining zones, and can be a result of interdislocation interactions and the generation of point defects [6, 11]. The mechanism of hydrogen-stimulated plastic strain localization is still under discussion [12]. Under the conditions of planar straining, the presence of interstitial hydrogen leads to a transition from the homogeneous plastic flow to localized straining in intense shear bands. According to the hypothesis of Terlink et al. [13], the hydrogen-stimulated plastic strain localization is related to the formation of pores in some layers of the strained material.

Acknowledgments. This study was supported in part by the Ministry of Education and Science of the Russian Federation within the framework of Program “Research and Pedagogical Personnel for Innovative Russia (2009–2013)” (project no. 14.740.11.0037 of 01.01.2010).

References

- [1] L.B. Zuev, V.I. Danilov and S.A. Barannikova: *Plastic Flow Macrolocalization Physics* (Nauka Publishers, Novosibirsk, 2008) (in Russian)
- [2] L.B. Zuev: *Ann. Phys.* Vol. 16, (2007), p. 286
- [3] L. D. Zuev, V. V. Gorbatenko, and S. N. Polyakov, in: *Proc SPIE* Vol. 4900 (2002), Part 2. p. 1197
- [4] P. Sofronis, Y. Liang, and N. Aravas: *J. Mech. A: Solids* Vol. 20 (2001), p. 857
- [5] I. V. Kireeva and Yu. I. Chumlyakov: *Phys. Met. Metallogr.* Vol. 108 (2009), p. 298
- [6] Yu. Yagodzinskyy, O. Tarasenko, S. Smuk, P. Aaltonen, and H. Hänninem: *Phys. Scr.* Vol. 94, (2001), p. 11
- [7] I. P. Chernov, A. M. Lider, and N. N. Nikitenkov, et al.: *Fiz. Mezomekh.* Vol. 9 (Spec. Issue), (2006), p. 11
- [8] E. I. Kuprekova, Yu. I. Chumlyakov, and I. P. Chernov: *Met. Sci. Heat. Treat.* Vol. 50 (5-6), (2008), p. 282
- [9] R. Berner and H. Kronmüller: *Plastische Verformung von Einkristallen* (Springer, Berlin, 1965).
- [10] S. L. Saltykov: *Stereometric Metallography* (Metallurgiya, Moscow, 1970).
- [11] V. G. Gavrilyuk and V. N. Shivanyuk: *Met. Sci. Heat. Treat.* Vol. 50 (5-6), (2008), p. 269
- [12] H. K. Birnbaum and P. Sofronis: *Mater. Sci. Eng. A* Vol. 176 (1994), p. 191
- [13] D. Terlink, F. Zok, J. D. Embry and M. F. Ashby: *Acta Met.* Vol. 36 (1988), p. 1213